Original Article

Evaluation and comparison of human absorbed dose of ^{90}Y-DOTA-Cetuximab in various age groups based on distribution data in rats

Ariandokht Vakili, Amir Reza Jalilian[1], Alireza Khorrami Moghadam[2], Maryam Ghazi-Zahedi[3], Bahram Salimi[1]

Department of Medical Radiation Engineering, Science and Research Branch, Islamic Azad University, [1]Radiopharmaceutical Research and Development Lab, Nuclear Science and Technology Research Institute, [2]Biomedical Physics and Engineering, Tehran University of Medical Sciences, [3]Faculty of science, K. N Toosi University of Technology, Tehran, Iran

Received on: 28.04.12 **Review completed on: 11.08.12** **Accepted on: 10.10.12**

ABSTRACT

The organ radiation-absorbed doses have been evaluated for humans in six age groups and both genders based on animal data. After intravenous administration of ^{90}Y-DOTA-Cetuximab to five groups of rats, they were sacrificed at exact time intervals (2, 24, 48, 72, and 96 h) and the percentage of injected dose per gram of each organ was calculated by direct counting from rat data. By using the formulation that Medical Internal Radiation Dose suggests, radiation-absorbed doses for all organs were calculated and extrapolated from rat to human. The total body absorbed dose for all groups was >22 mGy due to pure β-emission of the applied radiopharmaceutical. The effective dose resulting from an intravenously injected activity of 100 MBq is 56.7 mSv for a 60-kg female adult and 60.3 mSv for a 73-kg male adult. The results demonstrated the usefulness of this method for estimation of β-absorbed dose in humans.

Key words: Absorbed dose, beta-particles, internal dosimetry, Yttrium-90

Introduction

Absorbed-dose calculations provide a scientific basis for evaluating the biologic effects associated with administered radiopharmaceuticals. In cancer therapy, radiation dosimetry supports treatment planning, dose–response analyses, predictions of therapy effectiveness, and completeness of patient medical records. Prediction of human absorbed dose based on animal studies provides valuable distribution data for evaluating the potential use of new radiotracers. Yttrium-90 is a pure β-emitter, so performing dosimetry studies is not possible by using single-photon emission tomography (SPECT) and/or positron emission tomography (PET).

According to the authors' recent project on the production and evaluation of antibodies labeled with therapeutic radioisotopes for radio immune theraphy (RIT) applications, the production of ^{90}Y-DOTA-Cetuximab was performed.

The use of radiolabeled monoclonal antibodies for the treatment of cancer necessitates the development of dosing schedules that minimize the exposure of healthy tissues to radiation while maximizing the radiation dose received by the tumor.[1] The goal of RIT is to deliver radiation in discrete amounts to tumor sites via a radionuclide that has been conjugated to an antitumor monoclonal antibody (mAb). ^{90}Y-Cetuximab is a ^{90}Y-labeled mAb that binds specifically to the extracellular domain of epidermal growth factor receptor (EGFR) on both normal and tumor cells, and competitively inhibits the binding of epidermal growth factor (EGF) and other ligands, such as transforming growth factor-alpha. Binding of Cetuximab to the EGFR blocks phosphorylation and activation of receptor-associated

Address for correspondence:
Ms. Ariandokht Vakili,
Department of Medical Radiation Engineering, Science and Research Branch, Islamic Azad University, Tehran, Iran.
E-mail: ad.vakili@srbiau.ac.ir

Access this article online	
Quick Response Code:	Website: www.jmp.org.in
	DOI: 10.4103/0971-6203.103609

kinesis, resulting in inhibition of cell growth, induction of apoptosis, and decreased matrix metalloproteinase and vascular endothelial growth factor production, resulting in localization of mAb to tumor sites where ^{90}Y emits β-radiation capable of killing cells adjacent to the target cell.[2,3] ^{90}Y is a good candidate for RIT. Its high incidence of β-emission optimizes the dose deposition within the targeted cells while its low incidence of photons emission minimizes the dose received by other organs.[4] It can be produced easily by an $^{90}Sr/^{90}Y$ generator, decays by emission of β-radiation with a maximum energy of 2.28 MeV to stable Zirconium-90, with a half-life of 64.1 h.[5-7]

In this work, a precise description of organ distribution has been used owing to a large amount of distribution data (source organs in dosimetry calculations); the human absorbed radiation dose was estimated based on distribution data for normal rats.

Materials and Methods

DOTA-mono-*N*-hydroxysuccinimide ester (DOTA-mono-NHS ester) was purchased from Macrocyclics. Amicon Ultera-15 filter (Millipore, MWCO 30000) was purchased from GE Healthcare Inc, Amersham place, Buckinghamshire, UK. All other chemicals were purchased from Aldrich Chemical Co, Gillingham, UK. Cetuximab was kindly provided by Merck Inc, Darmstadt, Germany. Radio-chromatography was performed by counting of Whatman No.1 using a thin-layer chromatography scanner, Bioscan AR2000, Paris, France. Animal studies were carried out in accordance with the United Kingdom Biological Council's Guidelines on the Use of Living Animals in Scientific Investigations, 2nd ed. All of the rats were male NMRI purchased from Pasteur Institute of Iran; in each group/interval, five rats, before being sacrificed, were kept at routine day/night light program and were kept under common rodent diet pellets. The animal tissue samples were counted using a Wallac 1220 Quantulus, Perkin Elmer, Ultra low-level liquid scintillation spectrometer, Turku, Finland, after sample preparation method instructed by the manufacturer.

^{90}Y (valence, +3) is obtained from the natural decay of its parent, ^{90}Sr ($t_{1/2}$, 28 years), which is in turn a product of ^{235}U fission in a nuclear reactor. ^{90}Y is separated radiochemically from ^{90}Sr using a series of precipitation and filtration steps[8] or using a series of strontium-selective chromatographic columns. ^{90}Y was produced by $^{90}Y/^{90}Sr$ generator developed at Nuclear Science and Technology Research Institute of Atomic Energy Organization of Iran.

Preparation of ^{90}Y-DOTA-Cetuximab

mAb labeling with ^{90}Y was achieved starting with chelate DOTA-NHS-ester as described previously. The antibody conjugate was labeled using an optimization protocol according to the literature reports.[9,10] Radiolabeling of DOTA-cetuximab with ^{90}Y was performed by adding approximately 1 mg of the conjugate to 37–74 MBq (1–2 mCi) of $^{90}YCl_3$ in 0.1 M ammonium acetate buffer, pH 5.5, followed by 24 h incubation at 37°C. The radiochemical purity of the resulting ^{90}Y-DOTA-cetuximab was determined by radio–thin-layer chromatography (RTLC). RTLC showed a radiochemical purity more than 92% (specific activity = 0.55 GBq/mg) followed by filtration through PD10 column. The stability of the radioconjugate was tested in the presence of human serum at 37°C.

Biodistribution studies of radiopharmaceutical

The distribution of ^{90}Y-DOTA-Cetuximab among tissues was determined in five groups of male normal rats. A volume of 0.1 ml of final ^{90}Y-DOTA-Cetuximab solution containing 3.7 MBq radioactivity (0.1-0.2 mg/ml IgG determined by UV spectrophotometric method) was injected into the dorsal tail vein. The animals were sacrificed by CO_2 asphyxiation (after anesthesia induction using propofol/xylazine mixture) at the exact time intervals (2, 24, 48, 72, and 96 h), and dissection was started by drawing blood from the aorta, followed by collecting heart, spleen, kidneys, liver, intestine, stomach, and skin samples.

Uptake measurement and analysis of animal data

In order to estimate the human absorbed dose, the initial step involves activity calculation. Consequently, the total amount of radioactivity injected into each rat was measured by counting the 1-ml syringe before and after injection in a dose calibrator with a fixed geometry. The samples were weighed and tissue uptakes were calculated as the percentage of injected dose per gram (%ID/g = %IA/g) by using a beta-scintillator detector. These measurements were tabulated as decay-corrected biodistributions in various organs and at a number of time points after injection of the radiolabeled material. All the organ activity measurements were normalized to the injected activity [Table 1]. The ^{90}Y activity concentration at time t, $C_{tissue}(t)$, was then calculated as the percentage of injected activity per gram of tissue (%IA/g) with equation (1):

$$\mathrm{Ctissue}(t) = \frac{A\,tissue(t)/M\,tissue}{A\,total} \times 100, \qquad \text{.....(1)}$$

where $A_{tissue}(t)$ is the ^{90}Y activity in the sample, M_{tissue} is the mass of the sample, and A_{total} is the total activity of ^{90}Y injected into the rat. The dosimetry estimates were based on a rat distribution study and the calculations were done in accordance with International Commission on Radiation Protection (ICRP) 103[11] and ICRP 106[12] recommendations.

To estimate the absorbed dose in human from the biokinetic results in the rat, we used a mass correction factor to account for the different ratios of organ to total body weights in the rat and in human. To first order, we assume

that the uptake in a given organ, in %IA, depends only on the ratio of organ mass divided by the total body mass.[13]. To correct for differences in this apportionment ratio between rat and human species, we can use equation (2), where:

$$CR = \frac{\left[\frac{Organ\,mass}{Total\,body\,mass}\right]human}{\left[\frac{Organ\,mass}{Total\,body\,mass}\right]Animal} \quad .....(2)$$

This process is essentially an organ correction factor (CR) for differences in relative perfusion between the rat (and other animal) model and the human subject. Usually the biokinetic data from the animals are provided as %IA/g, which simplifies this conversion for dose estimation as the rat organ mass is included in the data set. These correction factors have been calculated by using data that are derived from ICRP and Medical Internal Radiation Dose (MIRD) pamphlet for six age groups and both genders[14] [Tables 2 and 3], so are often sizeable and should be applied when using animal data to predict human results.

Dose estimation in humans from rats' biodistribution data

The activity and concentration of the radiopharmaceutical in all major source organs and spaces in the body must be determined for the dose calculation step. Activity calculation was performed by using a mathematical biodistribution model which generated non-decay corrected time activity curves for the source organs including blood, lungs, kidneys, spleen, liver, bone, muscle, skin, and stomach for all groups. For each organ, there is a plot of the distribution data which in points fit to a single exponential equation except for the heart and blood (because it was multi-exponential), by least-squares linear regression that presenting the subtraction between input rate and output rate of radiopharmaceutical to individual organs, fitted a mono-exponential curve. The data points representing the percentage-injected dose (%ID/organ) were created and fitted to a mono-exponential, a bi-exponential, or an uptake-and-clearance curve. The cumulated source activity (A_h) is calculated for each organ according to equation (3) which is presented in the Medical Internal Radiation Dose (MIRD) No. 11:[15]

$$\tilde{A}h = \int_{t1}^{\infty} Ah(t)dt \quad .....(3)$$

The activities were determined by integration of mathematical equations that were obtained based on %ID/g for each organ during interval times from 2 to 96 h [Table 4].[16] The rat data were assumed to approximate the biokinetics in human.

A fundamental equality generally assumed in the estimation of organ doses is the familiar equation (4):

$$D_{t\leftarrow s}[rad] = S_{t\leftarrow s}\left[\frac{rad}{\mu Ci - h}\right].\tilde{A}[\mu Ci\text{-}h], \quad .....(4)$$

where $S_{t\leftarrow s}$ is a rectangular matrix giving the dose to a target organ t per unit time activity in a source organ S.[16,17] Conceptually, equation (4) separates the analytic process into two segments. Given the radionuclide, S refers purely to geometric factors. The cumulated activity $\tilde{A}_h$ is the area under the curve of activity (A_S) versus time. Traditional dimensions, rad/(μCi-h) for S, are changed to cGy/MBq-h for SI units. Notice that D and $\tilde{A}$ are column vectors in this formula; their various elements refer to the source and target organs for a specified radionuclide.

Properties of the S matrix

One may logically separate S factor into S_{np} and S_p parts; these refer to so-called non-penetrating (np) and penetrating (p) radiation given off by the radionuclide of interest. Typically, the user assigns charged particle radiation to the former category and gamma and X-rays to the latter. Some emitters, such as ^{90}Y that were used in this work, are purely of the charged-particle type; these are of considerable interest in RIT due to the reduction in ambient radiation levels during therapy procedures, so S_{np} is the only part of S factor for this radioisotope[18] (equation (5):

$$S_{t\leftarrow s} = \Sigma\Delta_i\Phi_{i\,t\leftarrow s} \quad .....(5)$$

When all dimensions of an organ t greatly exceed the rang of the electron, i.e., the source and target organ are the same, equation (6)

$$\Phi_{t\leftarrow s} = \frac{\varphi_{t\leftarrow s}}{m} = \frac{1}{m} \quad .....(6)$$

is assumed to hold, where m is the mass of target organ. The source and target organ are well separated,

$$\Phi_{t\leftarrow s} = 0 \quad .....(7)$$

The exceptions to the above general rules for bone, marrow, and organ with walls are thoroughly discussed, and the precise values of S factors are presented in tables of the MIRD pamphlet No. 11[15] for over 110 radionuclides like ^{90}Y. Methods used for calculation of radiation-absorbed dose to the human normal organs and whole body are by those recommended by the MIRD Committee of the Society of Nuclear Medicine.[19-21]

Results

Biodistribution of ^{90}Y-DOTA-cetuximab in rats at five different time intervals, 2, 24, 48, 72, and 96 h, post-injection are shown in Table 1. At 2 h post-injection, the activity is mainly in the blood, which is in agreement with the other reported labeled antibodies, such as ^{64}Cu-

DOTA-Cetuximab,[7] ^{89}Zr-Cetuximab,[22] and ^{177}Lu-Cetuximab.[23] But the activity of the stomach, muscle, and intestine is rather low. But retention of radiopharmaceutical in the blood at all five time interval was significantly higher in our system indicating the long circulation lifetime of the antibody. High uptake in the lung, blood, and spleen which have EGFR expression was observed. Lung activity concentration was 1.18 ± 0.005 injected dose per gram-ID g/1% at 72 h and 1.23 ± 0.004 at 96 h post-injection, demonstrating the high EGFR expression. The liver also had prominent radioactivity accumulation, with an uptake of 2.19 ± 0.002 ID/g% at 24 h post-injection [Table 1].

The more conservative assumption that, it seems all ^{90}Y-DOTA-Cetuximab leaves the body due to natural decays would have been too conservative for organs with rapid clearance, such as the brain, kidney, skin, and muscle. Time–activity curves without decay correction are shown in Figure 1.

The radiation-absorbed organ doses estimated in humans according to the biological data from the rat study are shown in Table 5.

A 100 MBq (2.5 mCi) injection of ^{90}Y-DOTA-Cetuximab into the human body might result in an estimated absorbed dose of 16.08 mGy for the total body of adult female, 17.32 mGy for adult male, 16.323 mGy for 15-year-old female, 16.956 mGy for 15-year-old male, 17.54 mGy for age 10 years, 17.67 mGy for age 5 years, 18.84 mGy for age 1 year, and 21 mGy for newborn, and the highest absorbed dose was in the liver for all groups, followed by the lungs, kidney, marrow, bone, and skin, which are shown in Table 5.

The radiation-absorbed dose to red marrow was estimated according to MIRD recommendation and using equations (8 and 9). Three source organs are generally assumed for estimating marrow dose in red marrow, bone, and residual body.[19]

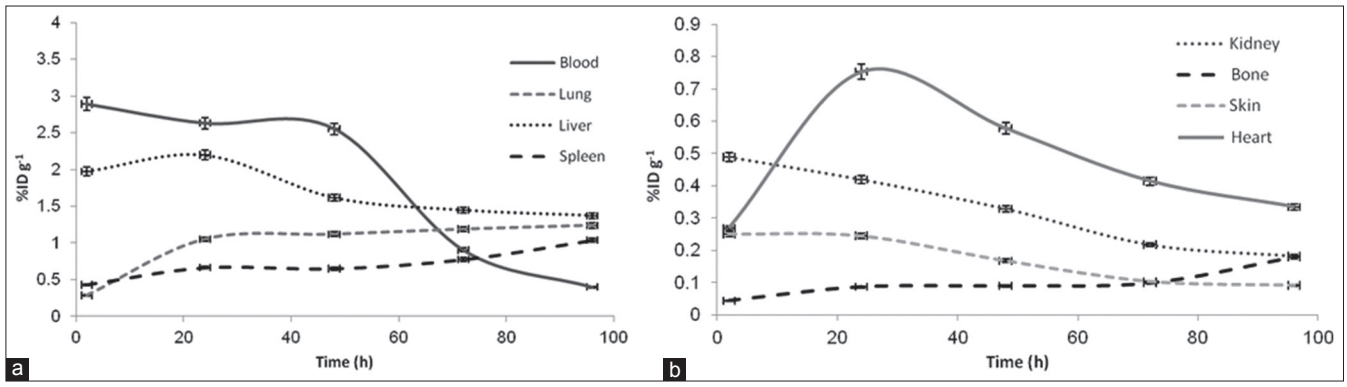

Figure 1: The non-decay corrected clearance curves from each organ of the rats (%ID/g, percentage of injected dose per gram) Mass correction factors were calculated in accordance with the MIRD committee of the Society of Nuclear Medicine and the ICRP recommendations for six age groups and both genders, and the mass of a normal rat was considered 0.28 kg, are presented in Table 2

Table 1: Biodistribution of ^{90}Y-DOTA-Cetuximab in normal rats 2–96 h post-injection

Organ/tissue	*Time (h)*[a]									
	2		*24*		*48*		*72*		*96*	
	Avg.	*SD*	*Avg.*	*SD*	*Avg.*	*SD*	*Avg.*	*SD*	*Avg.*	*SD*
Blood	2.88	0.004	2.63	0.005	2.55	0.03	0.74	0.004	0.397	0.004
Heart	0.26	0.016	0.753	0.02	0.58	0.017	0.414	0.03	0.334	0.03
Lung	0.28	0.009	1.05	0.007	1.12	0.005	1.185	0.005	1.237	0.008
Stomach	0.12	0.008	0.229	0.001	0.126	0.01	0.069	0.01	0.105	0.01
Colon	0.15	0.002	0.19	0.008	0.133	0.002	0.1	0.008	0.098	0.009
Intestine	0.16	0.011	0.123	0.009	0.04	0.008	0.094	0.009	0.052	0.01
Liver	1.97	0.01	2.2	0.002	1.61	0.001	1.45	0.02	1.37	0.002
Spleen	0.61	0.03	0.66	0.007	0.65	0.007	0.77	0.016	1.038	0.0018
Kidney	0.48	0.18	0.42	0.008	0.328	0.008	0.217	0.001	0.182	0.001
Muscle	0.0261	0.00	0.09	0.027	0.037	0.003	0.02	0.03	0.046	0.02
Sternum	0.066	0.03	0.09	0.025	0.124	0.016	0.138	0.02	0.124	0.02
Bone	0.004	0.17	0.16	0.01	0.109	0.001	0.198	0.00	0.278	0.06
Skin	0.025	0.034	0.24	0.03	0.167	0.003	0.102	0.02	0.091	0.007
Brain	0.016	0.007	0.039	0.01	0.031	0.003	0.006	0.001	0.013	0.005

[a]Data are presented as mean±SD and the mean value as the percentage of administered activity per gram

$$D_{rm} = D_{rm \leftarrow rm} + D_{rm \leftarrow bone} + D_{rm \leftarrow RB} \quad .....(8)$$

Bone as a source organ consists of two parts, trabecular bone and cortical bone.[14] In order to estimate marrow dose, one can use the blood concentration curve as a surrogate for the marrow concentration curve.[25] Instead of a direct correspondence, the marrow $\tilde{A}$ value is set equal to a fraction (f) of the blood curves $\tilde{A}$:[19]

$$\tilde{A}_{rm \leftarrow rm} = f \tilde{A}_{blood}[M_{marrow}/M_{blood}] \quad .....(9)$$

Physically, this relationship is an attempt to correct, to the lowest order, for the mass difference between the whole blood and red marrow. Values for the *f* factor have been estimated to lie between 0.2 and 0.4; a most probable value of 0.34–0.36 has been determined by Sgouros.[26]

The estimated effective doses to the whole body of all groups resulting from an intravenously injected activity of 100 MBq are presented in Table 5, the calculations were made in accordance with MIRD/ICRP 106 recommendations.[27]

It is worth mentioning that the radiation-absorbed dose to the red marrow of the rats is significantly high in comparison with other organs. (Calculations were performed using Macey *et al.*'s report, 1995.)[28] Therefore, it is necessary to attend to the marrow dose in each treatment planning based on RIT.

Comparison of the absorbed dose organs among the six age groups is presented in Figure 2. Also, a similar comparison is performed for both genders, which is shown in Figure 3.

Discussion

Recent trends in radionuclide therapy with radiolabeled antibodies and bone-seeking radiopharmaceuticals have promoted renewed interest in providing more accurate radiation-absorbed dose estimates. A wide range of radionuclides attached to a variety of targeting agents have been used in these trials. For many protocols, radiation-absorbed dose estimates are relied on to decide whether a patient should proceed to therapy and for prescribing the amount of activity that should be administered. The motivation for this work is the provision of absorbed dose estimates for individual patients within the limitations of methodology. Although the S values recommended by ICRP 62[29] and MIRD Pamphlet 11[15] have been used to provide the framework for radiation-absorbed dose estimates for human base on distribution data from small animals such as rats, more accurate methods are required for radionuclide therapy procedures. In this investigation, biodistribution of radioimmunoconjugate in rat model showed that it was mostly accumulated in lungs, which were the major organs of accumulation entirely in the study, as shown in Table 1. This is in agreement with the previous reports.[30] The lung to blood activity concentration ratio was about 1.68 at 72 h

Table 2: Standard masses (kg) according to ICRP 89[24] and mass correction factors

Age	*Adult*		*15 years*		*Newborn*	*1 year*	*5 years*	*10 years*
G	*M*	*F*	*M*	*F*				
Mass	73	60	56	53	3.5	10	19	32
CR	0.0038	0.0046	0.005	0.00528	0.08	0.028	0.014	0.0875

Table 3: Organs masses (g) according to ICRP 89[22]

Organ	*Adult*		*15 years*		*10 years*	*5 years*	*1 year*	*Newborn*
	Female	*Male*	*Female*	*Male*				
Blood	4100	5600	3500	4800	2500	1500	530	290
Heart	250	330	220	230	140	85	50	20
Lung	420	500	290	330	210	125	80	30
Stomach	140	150	120	120	85	50	20	7
Colon	145	150	122	122	85	49	20	7
Intestine	600	650	520	520	370	220	85	30
Liver	1400	1800	1300	1300	830	570	330	130
Spleen	130	150	130	130	80	50	29	9.5
Kidneys	275	310	240	250	180	110	70	25
Muscle	17,500	29,000	17,000	24,000	11,000	5600	1900	800
Sternum	121	162	107	124	71	38	20	7
Bone	7800	10500	7180	7950	4500	2430	1170	370
Marrow	900	1170	1000	1080	630	340	150	50
Skin	2300	3300	1700	2000	820	570	350	175
Brain	1300	1450	1300	1420	1220	1180	950	380

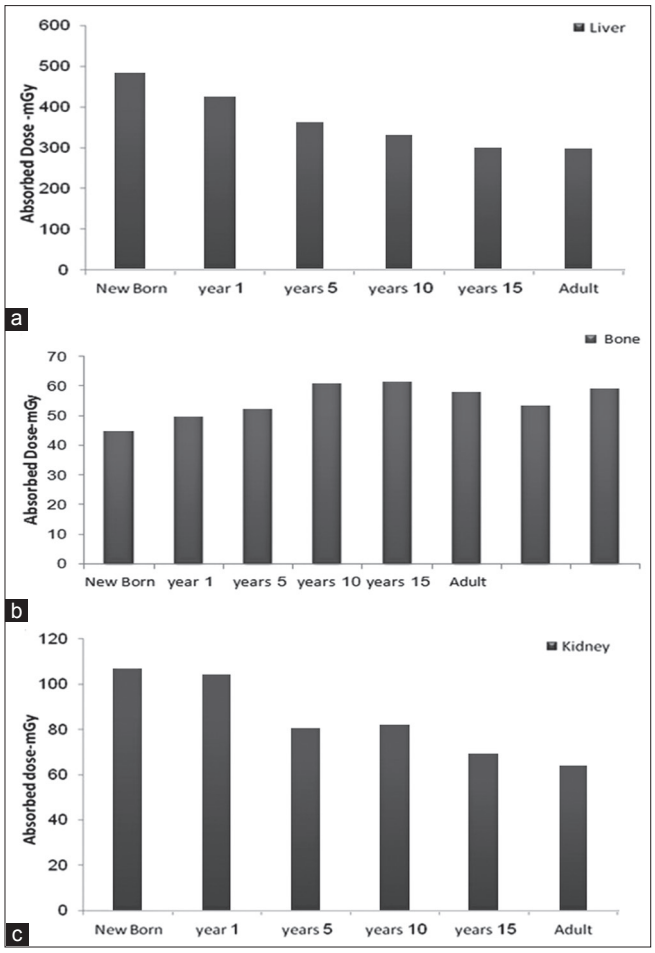

Figure 2: Comparison of absorbed dose among the six age groups: (a) liver, (b) bone, (c) kidney

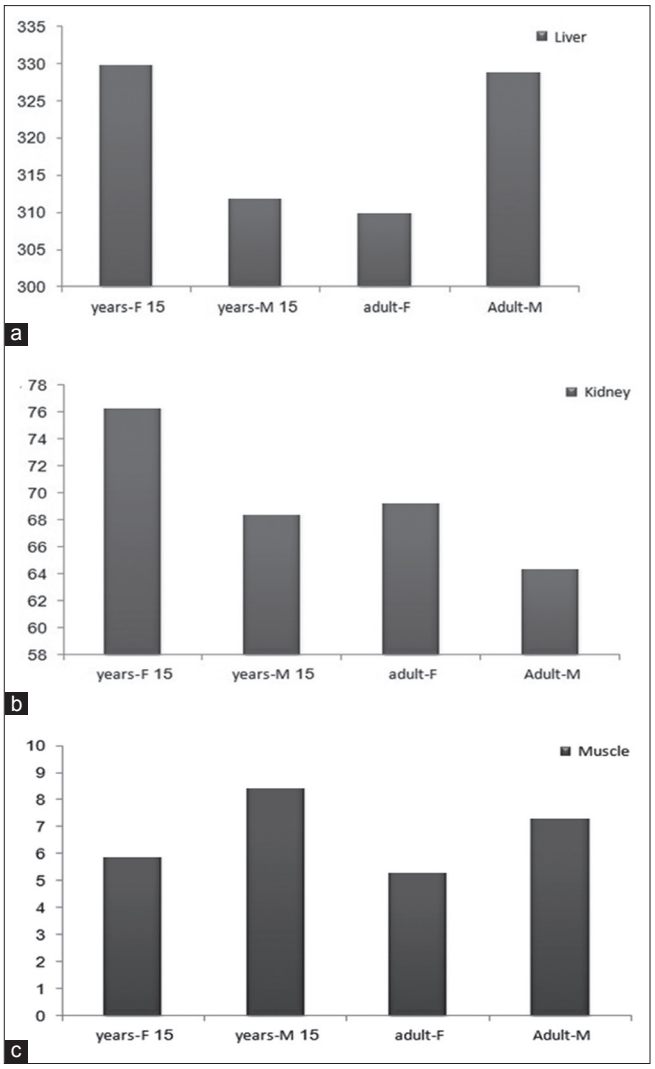

Figure 3: Comparison of absorbed dose between two genders: (a) liver, (b) kidney, (c) muscle

and up to 3.15 at 96 h post-injection. The lungs to muscle ratios were more than 30 at 72 and 96 h post-injection.

The present study estimated the dosimetry of ^{90}Y-DOTA-Cetuximab based on the generation of a mathematical biodistribution model. In radiological physics, a model of animal is required in the estimation of absorbed radiation dose. This follows from the need to perform integration of normal organ curves out to many physical half-lives. By using only physical decay or some crude form of extrapolation from the last data point(s), the investigator does not effectively understand the long-term course of the data. The same difficulty holds for the estimation of activity values between data points as taken (i.e., the model also provides better interpolation). As the physiological model, one may consider a separate multi-exponential representation for each of the various blood and normal organs. In this open model strategy, there is no explicit relationship between the various sets of exponentials from one organ to another as these fitting processes go on in isolation. This type of solution has certain justification as Laplace Transform analysis shows that linear modeling leads to a set of linear differential equations whose solutions are indeed combinations of various exponential functions.[31] In practice, it may be difficult, however, to fit more than two exponential functions to any organ curve. For one thing, only a single exponential solution is unique. Solutions involving multiple exponential functions have different results depending upon the starting conditions for the modeling algorithm used.

Residence time were calculated using animal and human data, and distribution of ratio of the animal results to human results were constructed for each extrapolation method, in this study, relative organ mass extrapolation method were used from overall four methods which represented by Sparks *et al*.[13] Relative organ mass scaling is based on the assumption that the uptake of activity in human organs is related to uptake in animal organs by a function of total body mass fractions of the organs in animals and human.[23] As a result of time points deficiency, relative organ mass extrapolation is more precise than physiological time extrapolation for this radiotracer.

Table 4: Distribution of ^{90}Y-DOTA-Cetuximab during 96 h for humans (MBq.s)

Organ	*Adult*		*15 years*		*10 years*	*5 years*	*1 year*	*Newborn*
	Female	*Male*	*Female*	*Male*				
Blood	2E7	1.78E7	1.74E7	2.27E7	2.07E7	1.98E7	1.4E7	2.19E7
Heart	1.38E5	1.51E5	1.39E5	1.39E5	1.47E5	1.43E5	1.68E5	1.92E5
Lung	8.23E5	8.1E5	6.53E5	7.03E5	7.83E5	7.4E5	9.5E5	1.02E6
Stomach	2.4E4	2.18E4	2.42E4	2.29E4	2.84E4	2.67E4	2.14E4	2.14E4
Liver	3.77E6	4E6	4.02E6	3.8E6	4.25E6	4.67E6	5.4E6	6.08E6
Spleen	1.36E5	1.3E5	1.57E5	1.48E5	1.6E5	1.6E5	1.85E5	1.74E5
Kidney	1.45E5	1.35E5	1.6E5	1.43E5	1.81E5	1.77E5	2.25E5	2.29E5
Muscle	1.06E6	1.45E6	1.18E6	1.58E6	1.26E6	1.03E6	7E5	8.4E5
Sternum	2.23E4	2.47E4	2.5E4	2.48E4	2.49E4	2.13E4	2.24E4	2.24E4
Bone	2.07E6	1.86E6	1.97E6	2.06E6	2.047E6	1.76E6	1.7E6	1.53E6
Marrow	1.57E6	1.43E6	1.7E6	1.78E6	1.82E6	1.52E6	1.37E6	1.3E6
Skin	6.09E5	7.22E5	5.69E5	5.76E5	4.13E5	4.59E5	5.64E5	8.06E5
Brain	6.12E4	5.63E4	7.02E4	7.26E4	1.09E5	1.69E5	2.37E5	3.11E5

Table 5: Organ dose (mGy) and effective dose (mSv)

Organ	*Adult*		*15 years*		*10 years*	*5 years*	*1 year*	*Newborn*
	Female	*Male*	*Female*	*Male*				
Liver	311	330	331	313	351	385	446	502
Lung	123	121	97	105	109	104	133	143
Spleen	11.29	10.77	13	12	13.22	13.22	15.34	14.36
Kidney	69.81	65	77	69	87	85	108	110
Stomach	7.39	6.54	7.39	6.88	8.53	8	6.42	6.42
Muscle	5.62	7.69	6.27	8.37	6.72	5.47	3.71	4.46
Skin	34.73	41.17	32.48	32.82	23.55	26.19	32.17	46
Bone	61.94	55.8	60.57	63.62	63.36	54.28	51.51	46.98
Marrow	148.43	134.12	154.41	161.98	163.48	137.47	126.96	118.75
Effective dose	56.7	60.3	66.8	55.1	62.9	60.9	50.4	69.1

The amount of radiation-absorbed dose in a human was calculated by determining the distribution in rats, obtaining the accumulated activity value by integration of multi-exponential mathematical model to each organ, multiplying by the ratio of organs to extrapolate to humans (using relative organ mass extrapolation), and then multiplying the converted rats' cumulative activity to the S factor table of ^{90}Y.[24] This procedure was also performed for all six age groups and both genders. The highest radiation-absorbed doses per unit-administered activity were calculated for liver, marrow, lungs, and bone in all groups for humans. It is worth mentioning that the radiation doses to the marrow were contributed by non-penetrating emissions in the marrow blood. The absorbed doses to the stomach and muscle were less than 9 mGy. The results in the present study represent a situation in which the extrapolation between animal data based on conventional methods may some over- or underestimate[16] the acceptable doses based on human data, and they were somewhat different from those obtained from the studies of rodents[32] as well as non-human primates.[33] This division may be particularly important if the absorbed dose estimations for humans are derived from animal models. In light of the results in this study, attention should be paid especially in situations where extrapolation between various animal species is more rational than extrapolation between animals and humans,[16] but other authors have demonstrated the usefulness of animal distribution as a model for absorbed dose estimations in humans.[34-36] Radiolabeled antibody is significantly accumulated in blood after 2 h. As observed, retention of radiopharmaceutical in the blood was significantly higher in our system, and finally at 72 h post-injection it gradually decreased. At the first 24 h post-injection, the radioactivity accumulates in the lungs due to the presence of EGFR receptors. A major problem about the described method is in selecting the time points, consistent with the mean biological half-life of antibody in humans and in rats.[15,37] It was anticipated that all the injected activity should be cleared from the main organs in up to 41 h, and therefore time points of 2, 24, 48, 72, and 96 h were selected. Comparison between absorbed doses of different age groups is shown in Figure 2 and it demonstrates that radiation-absorbed dose is different due to the biological differences and masses. The amount of absorbed dose for newborn and lower ages in most of the organs is significantly higher, and also this disparity in bone is as a result of skeletal system abortion in newborn, 1 year, and 5 years, at 10 years the amount of absorbed dose are equal with 15 years and

adult. The newborn and children are more sensitive to radiation, so administration of radiopharmaceuticals is impermissible for them. Also, comparison between both genders demonstrates that ^{90}Y-DOTA-Cetuximab is a sex-dependent radiopharmaceutical, due to the difference between the amount of absorbed dose, especially in liver, bone, and kidney. The difference between the absorbed doses in some organs is caused by different hormones secreted in both genders. Considering that ^{90}Y-DOTA-Cetuximab is a therapeutic radiopharmaceutical which emitted just β-particles and performing dosimetry according to the MIRD method is a way for predicting therapeutic dose in radioimmunotherapy (RIT).

Conclusion

Although mature, the field of radiopharmaceutical dosimetry is by no means senescent. Continued development of therapeutic applications, including use of radiolabeled monoclonal antibodies, presents significant challenges to the dosimetrist, as the traditional models of activity–that is, activity uniformly distributed in source organs, which irradiate target organs uniformly–no longer apply. In addition, the development of radiolabeled molecular probes of biologic function will also necessitate further developments in dosimetry to ensure their safe use in research.

Radiation dosimetry for ^{90}Y-DOTA-Cetuximab was estimated for humans based on the distribution data of ^{90}Y-DOTA-Cetuximab in normal rats. Previous studies have demonstrated the usefulness of animal distribution as a model for absorbed dose estimations in humans. The distribution of ^{90}Y-DOTA-Cetuximab in rats demonstrated high lung uptake and low muscle and spleen uptake. Although further dosimetry work should be performed on humans as ^{90}Y-DOTA-Cetuximab becomes useful in the clinic, these estimates can be used to predict potential absorbed doses in humans and for planning human studies.

The MIRD schema has provided an effective, uniform approach to the traditional issues of radiopharmaceutical dosimetry, and it will continue to form the foundation for enhanced dosimetry applications.

References

1. Ferl GZ, Kenanova V, Wu AM, DiStefano JJ. A two-tiered physiologically based model for dually labeled single-chain Fv-Fc antibody fragments. Mol Cancer Ther 2006;5:1550-8.
2. Wild R, Fager K, Flefleh C, Kan D, Inigo I, Castaneda S, *et al*. Cetuximab preclinical antitumor activity (monotherapy and combination based) is not predicted by relative total or activated epidermal growth factor receptor tumor expression levels. Mol Cancer Ther 2006;5:104-13.
3. Niu G, Sun X, Cao Q, Courter D, Koong A, Le GT, *et al*. Cetuximab-Based Immunotherapy and Radioimmunotherapy of Head and Neck Squamous Cell Carcinoma. Clin Cancer Res 2010;16:2095-105.
4. Deshpande SV, DeNardo SJ, Kukis DL, Moi MK, McCall MJ, DeNardo GL, *et al*. Yttrium-90-labeled monoclonal antibody for therapy bifunctional chelating agent: Labeling by a new macrocycic. J Nucl Med 1990;31:473-9.
5. Cremonesi M, Ferrari M, Grana CM, Vannazi A, Stabin M, Bartolomei M, *et al*. High-dose radioimmunotherapy with 90Y-ibritumomab tiuxetan: Comparative dosimetric study for tailored treatment. J Nucl Med 2007;48:1871-9.
6. Stabin MG, da Luz LC. New decay data for internal and external dose assessment. Health Phys 2002;83:471-52.
7. Eiblmaier M, Meyer LA, Watson MA, Fracasso PM, Pike LJ, Anderson CJ. Correlating EGFR Expression with Receptor-Binding Properties and Internalization of ^{64}Cu-DOTA-Cetuximab in 5 Cervical Cancer Cell Lines. J Nucl Med 2008;49:1472-9.
8. Bray L, Wester DW, Inventors. Battelle Memorial Institute, assignee. Method of separation of yttrium-90 from strontium-90. U.S. Patent. 1996;5:512,256.
9. Fisher DR, Shen S, Meredith RF. MIRD Dose Estimate Report No. 20: Radiation Absorbed Dose Estimates for 111In- and 90Y-Ibritumomab Tiuxetan. J Nucl Med 2009;50:644-52.
10. Pandey U, Mukherjee A, Sarma HD, Das T, Pillai MR, Venkatesha M. Evaluation of 90Y-DTPA and 90Y-DOTA for potential application in intra-vascular radionuclide therapy. Appl Radiat Isotopes 2002;57:313-8.
11. ICRP, 2007. The 2007 Recommendations of the International Commission on Radiological Protection. ICRP Publication 103. Ann. ICRP 37 (2-4).
12. ICRP, 2008. Radiation Dose to Patients from Radiopharmaceuticals - Addendum 3 to ICRP Publication 53. ICRP Publication 106. Ann. ICRP 38 (1-2).
13. Sparks RB, Aydogan B. Comparison of the effectiveness of some common animal data scaling techniques in estimating human radiation dose. In: Int. Radiopharmaceutical Dosimetry Sym. 6th ed. In: Stelson AT, Stabin MG, Sparks RB. Editors. Oak Ridge, TN: Oak Ridge Associated Universities; 1996. p. 705-16.
14. Peters JM, Boyd EM. Organ weights and water levels of the rat following reduced food intake. J Nutr 1996;90:354-60.
15. Snyder WS, Ford MR, Warner GG, Watson SB. 'S' absorbed dose per unit cumulated activity for selected radionuclides and organs. MIRD Pamphlet No. 11. New York, NY: Society of Nuclear Medicine; 1975.
16. Loevinger R, Berman MA. A Revised Schema for Calculating the Absorbed Dose from Biologically Distributed Radionuclides" in MIRD Pamphlet No. 1 Revised. New York: Society of Nuclear Medicine, 1976.
17. Loevinger R, Budinger TF, Watson EE. MIRD Primer for Absorbed Dose Calculations, Revised Edition. New York: Society of Nuclear Medicine; 1991.
18. Shanehsazzadeh S, Jalilian AR, Sadeghi HR, Allahverdi M. Determination of Human absorbed dose of 67Ga-DTPA-ACTH based on distribution data on rats. Radiat Prot Dosim 2009;134:79-86.
19. Macey DJ, Williams LE, Breitz HB, Liu A, Johnson TK, Zanzonico PB. A primer for radio immune therapy and radionuclide therapy. AAPM REPORT NO. 71; 2001.
20. International Commission on Radiation Units and Measurements. Methods of assessment of absorbed dose in clinical use of radionuclides. ICRU Publication Report No.32 Washington, DC: ICRU; 1979.
21. National Council on Radiation Protection and Measurements. The experimental basis for absorbed dose calculations in medical uses of radionuclides. Report No. 83 Bethesda, MD: National Council on Radiation Protection and Measurements; 1985.
22. Loevinger R, Budinger TF, Watson EE. MIRD Primer for Absorbed Dose Calculations; New York: Society of Nuclear Medicine, Inc; 1988.
23. Aerts HJ, Dubois L, Perk L, Vermaelen P, van Dongen G, Wouters BG, *et al*. Disparity Between *In Vivo* EGFR Expression and 89Zr-Labeled

Cetuximab Uptake Assessed with PET. J Nucl Med 2009;50:123-31.
24. Valentin J. Basic Anatomical and Physiological Data for Use in Radiological Protection: Reference Values ICRP publication 89; 2002.
25. Siegel JA, Wessels EE, Watson MG, Stabin HM, Vriesendorp EW, Bradley CC, *et al*. "Bone marrow dosimetry and toxicity in radioimmunotherapy." Antibod Immunoconj Radiopharm 1990;3:213-33.
26. Sgouros, G. Bone marrow dosimetry for radioimmunotherapy: Theoretical considerations. J Nucl Med 1993;34:689-94.
27. ICRP, Radiation Dose to Patients from Radiopharmaceuticals - Addendum 3 to ICRP Publication 53. ICRP Publication 106. Ann. ICRP 38 (1-2); 2008.
28. Macey DJ, DeNardo SJ, DeNardo GL, DeNardo DA, Shen S. Estimation of radiation absorbed doses to the red marrow in radioimmunotherapy. Clin Nucl Med 1995;20:117-25.
29. ICRP. Radiological protection in biomedical research. Also includes Addendum 1 to ICRP Publication 53, Radiation dose to patients from radiopharmaceuticals, and a summary of the current ICRP principles for protection of the patient in diagnostic radiology. ICRP Publication 62. Ann. ICRP 22(3). Oxford: Elsevier Science Ltd.; 1993.
30. DeGrado TR, Reiman RE, Price DT, Wang S, Coleman RE. Pharmacokinetics and radiation dosimetry of 18F-fluorocholine. J Nucl Med 2002;43:92-6.
31. Wagner JG. Fundamentals of Clinical Pharmacology. Hamilton, IL: Drug Intelligence Publications Inc.; 1975. p. 231-46.
32. Milenic DE, Wong KJ, Baidoo KE, Ray GL, Garmestani K, Williams M, *et al*. Cetuximab: Preclinical evaluation of a monoclonal antibody targeting EGFR for radioimmunodiagnostic and radioimmunotherapeutic applications. Cancer Biother Radiol 2008;23:619-31.
33. Wilson AA, Ginovart N, Hussey D, Meyer J, Houle S. *In vitro* and *in vivo* characterization of 11C-BASE: A probe for *in vivo* measurements of the serotonin transporter by positron emission tomography. Nucl Med Biol 2002;29:509-15.
34. Tipre DN, Lu JQ, Fujita M, Ichise M, Vines D, Innis RB. Radiation dosimetry estimates for the PET serotonin transporter probe 11C-DASB determined from whole-body imaging in non-human primates. Nucl Med Commun 2004;25:81-6.
35. Schmitt A, Bernhardt P, Nilsson O, Ahlman H, Kölby L, Schmitt J, *et al*. Biodistribution and dosimetry of 177Lu-labeled [DOTA0, Tyr3] octreotate in male nude mice with human small cell lung cancer. Cancer Biother Radiopharm 2003;18:593-9.
36. De Jong M, Breeman WA, Bernard BF, Baker BK, Schaar M, Van Gameren A, *et al*. [177Lu-DOTA0, Tyr3] octreotate for somatostatin receptor-targeted radionuclide therapy. Int J Cancer 2001;92:628-33.
37. Vincenzi B, Santini D, Tonini G. New issues on cetuximab mechanism of action I epidermal growth factor receptor–negative colorectal cancer: The role of vascular endothelial growth factor. J Clin Oncol 2006;24:1957-8.

How to cite this article: Vakili A, Jalilian AR, Moghadam AK, Ghazi-Zahedi M, Salimi B. Evaluation and comparison of human absorbed dose of ^{90}Y-DOTA-Cetuximab in various age groups based on distribution data in rats. J Med Phys 2012;37:226-34.

Source of Support: Nil, **Conflict of Interest:** None declared.